Differential binding of proteins to peroxisomes in rat hepatoma cells: unique association of enzymes involved in isoprenoid metabolism

Sita D. Gupta,* Ryan S. Mehan,* Terese R. Tansey,* Hua-Tang Chen,[1,*] Gertrud Goping,[†] Israel Goldberg,[2,*] and Ishaiahu Shechter[3,*]

From the Department of Biochemistry and Molecular Biology* and Department of Anatomy and Cell Biology,[†] F. Edward Hébert School of Medicine, Uniformed Services University of the Health Sciences, Bethesda, MD 20814-4799

Abstract **Farnesyl diphosphate synthase (FPPS: EC2.5.1.10), a key enzyme in isoprenoid metabolic pathways, catalyzes the synthesis of farnesyl diphosphate (FPP) an intermediate in the biosynthesis of both sterol and non-sterol isoprenoid end products. The localization of FPPS to peroxisomes has been reported (**Krisans, S. K., J. Ericsson, P. A. Edwards, and G. A. Keller. **1994.** ***J. Biol. Chem.*** 269: **14165–14169). Using indirect immunofluorescence and immunoelectron microscopic techniques we show here that FPPS is localized predominantly in the peroxisomes of rat hepatoma H35 cells. However, the partial release of 60–70% of cellular FPPS activity is observed by selective permeabilization of these cells with digitonin. Under these conditions, lactate dehydrogenase, a cytosolic enzyme, is completely released whereas catalase, a known peroxisomal enzyme, is fully retained. Digitonin treatment of H35 cells differentially affects the release of other peroxisomal enzymes involved in isoprenoid metabolism. For instance, mevalonate kinase and phosphomevalonate kinase are almost totally released (95% and 91%, respectively), whereas 3-hydroxy-3-methylglutaryl-CoA reductase is fully retained. Indirect immunoflourescence studies indicate that FPPS is localized in peroxisomes of Chinese hamster ovary (CHO)-K1 cells but is dispersed in the cytosol of ZR-82 cells, a mutant that lacks peroxisomes. Unlike in H35 cells, FPPS is completely released upon digitonin permeabilization of CHO-K1 and ZR-82 cells. In contrast, under the same permeabilization conditions, catalase is fully retained in CHO-K1 cells but completely released from ZR-82 cells. These studies indicate that FPPS and other enzymes in the isoprenoid biosynthetic pathways, involved in the formation of FPP, are differentially associated with peroxisomes and may easily diffuse to the cytosol. Based on these observations, the significance and a possible regulatory model in the formation of isoprenoid end-products are discussed.**—Gupta, S. D., R. S. Mehan, T. R. Tansey, H-T. Chen, G. Goping, I. Goldberg, and I. Shechter. **Differential binding of proteins to peroxisomes in rat hepatoma cells: unique association of enzymes involved in isoprenoid metabolism.** ***J. Lipid Res.*** **1999.** 40: **1572–1584.**

Supplementary key words peroxisomes • cholesterol • isoprenoids • immunofluorescence • cellular permeabilization • farnesyl diphosphate synthase • catalase

Biosynthetic pathways utilizing isoprene units produce an extraordinarily diverse number of metabolites in addition to cholesterol. The enzymes that produce cholesterol and other isoprenoids are distributed in different subcellular compartments (1). The conversion of acetyl-CoA to 3-hydroxy-3-methylglutaryl-CoA (HMG-CoA) occurs in the cytosol. The further conversion of HMG-CoA to mevalonate catalyzed by HMG-CoA reductase occurs not only in the endoplasmic reticulum (ER) but also in the matrix of the peroxisomes (2, 3). Recent studies by Engfelt et al. (4) identified two HMG-CoA reductase proteins in Chinese hamster ovary (CHO) cells, a 97 kDa species localized in the ER and a 90 kDa isozyme in peroxisomes (4). Studies by several investigators have shown that the enzymes mevalonate kinase (5, 6), phosphomevalonate kinase (7), diphosphomevalonate decarboxylase (7), and isopentenyl diphosphate dimethylallyl diphosphate (IPP) isomerase (8) which produce intermediates for the synthesis of farnesyl diphosphate (FPP), and FPP synthase (FPPS) (9), are localized in peroxisomes (1). Based on these findings it was proposed that the conversion of mevalonate to FPP may occur exclusively in peroxisomes (5–9).

It was demonstrated that squalene synthase is localized exclusively in the ER and thus, the conversion of FPP to squalene occurs there (10). Studies by S. Krisans (1) on the conversion of squalene and dihydrolanosterol to cholesterol indicated that the conversion of squalene to choles-

Abbreviations: BSA, bovine serum albumin; DTT, dithiothreitol; ER, endoplasmic reticulum; FPP, farnesyl diphosphate; FPPS, farnesyl diphosphate synthase; GPP, geranyl diphosphate; HMG-CoA, 3-hydroxy-3-methylglutaryl-coenzyme A; LDH, lactate dehydrogenase; IPP, isopentenyl diphosphate; PBS, phosphate-buffered saline.

[1] Present address: Experimental Immunology Branch, National Cancer Institute, National Institutes of Health, Bethesda, MD 20895.

[2] Present address: Department of Molecular Genetics and Biotechnology, The Hebrew University-Hadassah Medical School, P.O. Box 12272, Jerusalem, Israel.

[3] To whom correspondence should be addressed.

terol occurs only in the ER. Peroxisomes do not appear to contain squalene epoxidase and oxidosqualene cyclase, the enzymes required for the conversion of squalene to lanosterol (1, 11). The presence of four enzyme activities that are involved in later steps of cholesterol production (dihydrolansterol oxidase, steroid-14-reductase, steroid-3-ketoreductase, and steroid-8-isomerase) in peroxisomes (11), supports a role for this organelle in the conversion of lanosterol to cholesterol.

FPP is an intermediate in the branch point of the isoprenoid biosynthetic pathway. It can be incorporated into either sterol or nonsterol end products: squalene, dolichols, coenzyme Q, the isoprenoid moiety of Heme A, and the (poly)isoprene moieties of prenylated G proteins (12). Thus, FPP is involved in both cellular growth and signaling (12, 13). The regulation of FPP formation and its further conversion to sterols has been extensively investigated (14–21). The significance of the subcellular localization of the enzymes involved in the biosynthesis and utilization of FPP is not well understood. As the liver is the major site of cholesterol production and has the highest number of peroxisomes (22), most of the biochemical studies on FPP biosynthesis have utilized rodent hepatic tissue or cultured cells.

The association of FPPS with peroxisomes may indicate that this organelle plays a central role in the regulation of growth and signaling. A group of human diseases related to inborn errors of metabolism such as Zellweger syndrome, neonatal adrenoleucodystrophy, and infantile Refsum syndrome are characterized by biochemical dysfunction and morphological abnormalities of peroxisomes (23). Cells isolated from Zellweger syndrome patients (24), as well as certain cultured cell models, are peroxisome-deficient, lacking a functional peroxisome assembly factor (PAF)-1 (25–29). The lack of peroxisomes in these cells correlates with lower amounts of peroxisomal matrix enzymes which results in the absence or reduced activity of independent peroxisomal pathways such as plasmologen biosynthesis, degradation of very long chain fatty acids, accumulation of bile acid intermediates, and low plasma cholesterol levels in these patients (23, 30). These cases underscore the important role of this subcellular compartment (23). For the study of peroxisomal deficiencies, several CHO-K1 cell lines with point mutations in PAF-1 have been isolated. Two of these lines (ZR-78 and ZR-82) lack normal peroxisomal functions and were shown to have the peroxisomal enzyme catalase dispersed in the cytosol (25, 29). In our present studies, we also utilized the ZR-82 line to assess the association of enzymes involved in the production of FPP with peroxisomes. Aboushadi and Krisans (31) have proposed that FPP is synthesized in the peroxisomes and then transported to other cellular compartments for further processing. Based on this and our earlier observations that squalene is produced in the ER (10), it is not clear how FPP is transported out of the peroxisomes to the ER for cholesterol production. To better understand the relationship between regulatory function and subcellular localization of enzymes involved in the cholesterol biosynthetic pathway, studies were undertaken to characterize the association of FPPS with peroxisomes. Both normal and peroxisome-deficient cell lines were used for these studies. Here, we report the results of immunological and biochemical studies that show unique characteristics of the association of several enzymes of FPP biosynthesis with peroxisomes.

MATERIALS AND METHODS

Materials

[4-^{14}C]isopentenyl diphosphate (IPP) (54.1 mCi/mmol) was purchased from DuPont NEN, and unlabeled IPP and geranyl diphosphate (GPP) were from Sigma. RS-[5-^{3}H]mevalonic acid (60 Ci/mmol) and R-[5-^{3}H]mevalonic acid monophosphate (60 Ci/mmol) were from ARC. Protease inhibitor cocktail tablets (Complete™) were purchased from Boehringer Mannheim. BCA protein assay reagents were from Pierce Chemical Co. Cell culture media were purchased from Life Technologies, Inc. Sheep anti-human catalase antibody was purchased from Accurate Chemical & Scientific Corporation (Westbury, NY). Fluorescein-conjugated donkey anti-rabbit IgG (H + L) antibody, rhodamine-conjugated donkey anti-sheep IgG (H + L) antibody, and normal donkey serum were purchased from Jackson ImmunoResearch Laboratories, Inc. (West Grove, PA). Goat anti-rabbit 15 nm gold-conjugated IgG (H + L), was purchased from Ted Pella, Inc. (Redding, CA). All other chemicals were from Sigma Chemical Co.

Cell culture and growth

The rat hepatoma H35 cells were maintained at 37°C in Dulbecco's modified Eagle's medium (DMEM) supplemented with 10% (v/v) fetal bovine serum, glutamine (0.292 mg/ml), penicillin (100 units/ml), streptomycin (100 μg/ml), and sodium pyruvate (1 mm). Wild-type CHO-K1 and the mutant ZR-82 cells were kindly provided by Dr. R. Thieringer (Merck Research Laboratories, Rahway, NJ) and were maintained at 37°C in Ham's F-12 growth medium containing 10% (v/v) fetal bovine serum, supplemented with glutamine (1.2 mm), penicillin (60 μg/ml), streptomycin (60 μg/ml), and insulin (0.51 μg/ml) (26). For HMG-CoA reductase assays, 24 h prior to permeabilization, H35 cells were transferred to the complete DMEM media supplemented with 10% lipid-depleted serum (LDS).

Enzyme assays

FPPS assay. FPPS was assayed as described previously (9) with some modifications. Reactions were carried out in 25 mm HEPES, pH 7.0, containing 2 mm $MgCl_2$, 1 mm DTT, 5 mm KF, 1% n-octyl β-glycopyranoside, 3.3 μm [4-^{14}C]IPP (18 Ci/mmol), and 18 μM GPP in a final volume of 150 μl. Reactions were started by the addition of 100 μg of cell lysate protein and incubated for 45 min at 37°C. The reactions were stopped by the addition of 150 μl 2.5 N HCl in 80% ethanol containing 100 μg/ml farnesol as a carrier. The samples were hydrolyzed for 30 min at 37°C to convert the FPP to farnesol and neutralized by the addition of 150 μl of 10% NaOH. The reaction product (farnesol) was extracted into 1 ml of n-hexane, and 200 μl of the organic phase was used for radioactivity counting. One unit of enzyme activity is defined as the amount of enzyme required to synthesize one pmole of FPP per min.

Mevalonate kinase assay. Mevalonate kinase was assayed as described (5, 6) with some modifications. The reaction buffer consisted of 100 mm phosphate buffer (pH 7.4), 15 mm ATP, 4 mm $MgCl_2$, 1 mm EDTA, 1 mm dithiothreitol, 13 mm CHAPS, and cell lysates in a final volume 400 μl. RS-[5-^{3}H]mevalonic acid (565 nmol) was added at a specific activity of 7858 dpm/nmol and

incubated at 37°C for 40 min. Reactions were terminated by boiling samples for 10 min. The reaction mixtures were loaded on AG 1-X8 formate (200–400 mesh) columns (2 ml). Columns were washed with 25 ml water, 50 ml 2 N formic acid (to elute unreacted substrate), and then 50 ml 4 N formic acid to elute the mevalonate-5-phosphate product. Three-ml fractions of effluent were collected and counted for radioactivity. One unit of enzyme activity is defined as the amount of enzyme required to synthesize 1 nmole of mevalonate-5-phosphate per min.

Phosphomevalonate kinase assay. The reaction conditions were the same as for mevalonate kinase except that instead of mevalonic acid, R-[5-^{3}H]mevalonic acid phosphate (17.52 nmol) was added at a specific activity of 1.267×10^4 dpm/nmol. The anion exchange columns were washed with 25 ml water, 50 ml of 4 N formic acid (to elute the substrate) and 50 ml of 0.8 M ammonium formate in 4 N formic acid to elute the diphosphorylated product (5, 9). One unit of enzyme activity is defined as the amount of enzyme required to synthesize one nmole of mevalonate diphosphate per min.

HMG-CoA reductase assay. HMG-CoA reductase was assayed essentially according to previous procedures (2, 32, 33). The samples were preincubated for 30 min at 37°C before the addition of substrate to ensure the inactivation of HMG-CoA lyase activity (2). The incubation mixture consisted of 15–60 μg of protein, 57 mM CHAPS, and reaction buffer (50 mM potassium phosphate, pH 7.4, 30 mM EDTA, 125 mM NaCl, and 10 mM DTT) in 130 μl final volume. The reaction was started by adding 20 μl substrate mixture containing 352 μM [^{14}C]HMG-CoA and 2.7 mM NADPH (final concentration) and 60,000 dpm of [^{3}H]mevalonate. The samples were incubated at 37°C for 30 min and the reaction was stopped by the addition of 20 μl of 125 mM mevalonic acid lactone in 6 N HCl. The samples were centrifuged and 100 μl of the protein-free samples was spotted on TLC plates and developed in benzene–acetone 1:1 (v/v) (32). The areas corresponding to mevalonate lactone were scraped off, the radioactive counts were measured, and the values were corrected for mevalonic acid recovery as described (32). One unit of enzyme activity is defined as the amount of enzyme required to synthesize one pmole of mevalonate lactone per min.

Lactate dehydrogenase assay. Lactate dehydrogenase was assayed according to a Sigma protocol, and catalase was assayed according to Baudhuim et al. (34) except that BSA was omitted from the assay buffer and the reaction was carried out at 25°C. Enzyme activities are expressed as standard units (μmol/min). Protein concentration was determined by the BCA method (Pierce Chemical Co.) using BSA as a standard.

Permeabilization of cells

Cells were permeabilized with digitonin essentially as described (7, 35) with Complete protease inhibitor cocktail in all the solutions. For time-course experiments, H35 cells were seeded at a density of 3×10^6 on 150-mm plates and grown to 70–80% confluency in complete Dulbecco's modified Eagle's medium containing 10% fetal bovine serum. Under these conditions there were approximately 1.5×10^7 cells per plate. On the day of the experiment, the media was removed and the plates were then washed twice with 10 ml of ice-cold KH buffer (50 mM HEPES, 110 mM potassium acetate, pH 7.2). The plates were transferred to ice and the cells were incubated in 20 ml KHM buffer (20 mM HEPES, 110 mM potassium acetate, 2 mM magnesium acetate, pH 7.2) containing 40 μg/ml digitonin (Fluka Biochemica), with a gentle shaking. At different time intervals, 1.5 ml digitonin solution was withdrawn and kept on ice. At the last time point, the entire digitonin solution was withdrawn and the cells were washed twice with 10 ml of ice-cold KH buffer containing protease inhibitors. These washes were combined and saved for enzyme assays. Under this procedure, the cells remain attached to the plates. After digitonin treatment and washings, 5 ml of PBS containing protease inhibitors was added to each plate and the cells were scraped off. This procedure was repeated and the cells were then collected by centrifugation for 10 min at 1000 rpm, suspended in 0.5 ml of the same solution, and sonicated three times for 15 sec. After centrifugation for 5 min at 14,000 rpm, the supernatant solutions (cell lysates) and the digitonin extracts (cell washes) were used for protein estimation and enzyme assays. Cells on control plates were treated with KHM buffer without digitonin and processed exactly the same way as the digitonin-treated cells. The amount of protein or enzyme activities retained in the cells from control plates was taken as 100%. In other permeabilization experiments, cells were treated exactly as mentioned above, except that they were incubated with buffer containing digitonin for the indicated time period and the washed cells were scraped in 0.5 ml of PBS containing protease inhibitors, lysed by sonicating twice for 10 sec, and directly assayed.

Generation of anti-FPP synthetase antibody

The peptide PQGQVDLGRYTEKRC, representing amino acids 179–192 of rat liver FPPS (36) with an additional C-terminal cysteine, used to conjugate the peptide to keyhole limpet hemocyanin (KLH), was synthesized by Biosynthesis, Lewisville, TX. Rabbit anti FPPS antiserum was prepared by the Pocono Rabbit Farm, Canadensis, PA, using standard immunization protocol. To confirm that the antiserum used in the present study detected FPPS, the enzyme was expressed in bacteria using an expression vector containing rat FPPS cDNA (provided by Dr. Peter Edwards, Dept. of Biological Chemistry, UCLA). The antiserum reacted with a single band of ~41 kDa on Western blots of lysates prepared from bacteria harboring the expression vector (see Fig. 5); no reaction was seen in lysates lacking the FPPS cDNA insert (data not shown). Western blots of lysates from H35 cells treated for 20 h with 10 μg/ml lovastatin to induce FPPS showed increased immumoreactivity in a band of ~41 kDa versus control cells (data not shown).

Western blot analyses

Thirty–100 μg of protein from each sample was electrophoresed on a 10% SDS-polyacrylamide gel (37) and transferred onto nitrocellulose membranes. Membranes were blocked in PBST (PBS containing 0.05% Tween 20) with 5% fat-free milk, and incubated with rabbit anti-rat FPPS antibody (1:3000 dilution) in PBST containing 1% BSA. The washed membranes were treated with goat peroxidase-labeled anti-rabbit antibody at a 1:5000 dilution. The blots were developed with the ECL reagents from Amersham.

Double labeled indirect immunofluorescence microscopy

Cells were plated on coverslips. After 24-h growth at 37°C, the growth medium was removed and cells were washed twice with PBS. For immunofluorescent labeling of the permeabilized cells, the cells on coverslips were first treated with digitonin buffer as mentioned above. The cells were then fixed with 4% (w/v) formaldehyde at room temperature for 20 min, treated with 0.2% Triton X-100 in PBS containing 1% BSA for 10 min, and incubated in 1% glycine in PBS solution for 10 min. Treated cells were incubated with protein-A agarose-purified anti-FPPS antibody (at a final dilution of 1:8000 in PBS containing 5% normal donkey serum) at room temperature for 60 min, washed 3×10 min and 1×15 min with PBST, and then incubated for 60 min with sheep anti-human catalase antibody (diluted 1:500). Cells on coverslips were washed as described above and then incubated with fluorescein-conjugated affinity-purified donkey anti-rabbit IgG (H+L) antibody (diluted 1:200) for 60 min followed by washings with PBST. The cells were then incubated for 60 min with rhodamine-conjugated donkey anti-sheep IgG (H + L) antibody at a final di-

lution of 1:200. After washing with PBST, the coverslips were mounted on microscope slides with Mowiol 4-88. Fluorescence microscopy was performed using a Bio-Rad Confocal Imaging System, MRC 600, equipped with a Zeiss Axiovert 35 microscope and a motorized Z drive. For quantitative measurements of immunofluorescence, images were taken at different focal planes, 0.5 microns apart. Fluorescein fluorescence (FPPS) was monitored using a 488 nm bandpass filter and rhodamine (catalase) was detected at 514 nm. Immunofluroscence is represented by pseudocolors generated by the computer using Superdraw and TIFFANY software.

Immunoelectron microscopy

Normal and permeabilized H35 liver cells were scraped into PBS containing protease inhibitors and collected by centrifugation at 1000 rpm for 5 min. The cells were fixed in 0.1 m Na-cacodylate buffer (pH 7.4) containing 2% sucrose, 4% paraformaldehyde, and 0.1% glutaraldehyde for 45 min at room temperature. After fixation, pellets were washed three times in 0.1 m Na-cacodylate buffer. Post-fixation with osmium tetroxide was avoided. The samples were dehydrated with a series of increased alcohol concentrations with 70% as the highest concentration, embedded in LR White, and polymerized under vacuum at 40°C as described previously (38). Ultrathin sections were cut with a Diatome knife on a Reichert ultra microtome at 90 nm thickness and collected on copper and nickel grids.

Immunolabeling of ultrathin sections on nickel grids was performed as described previously (38). The first antibody was polyclonal rabbit anti-FPPS antibody used at a dilution of 1:500. Secondary antibody used was gold (mean diameter = 15 nm)-

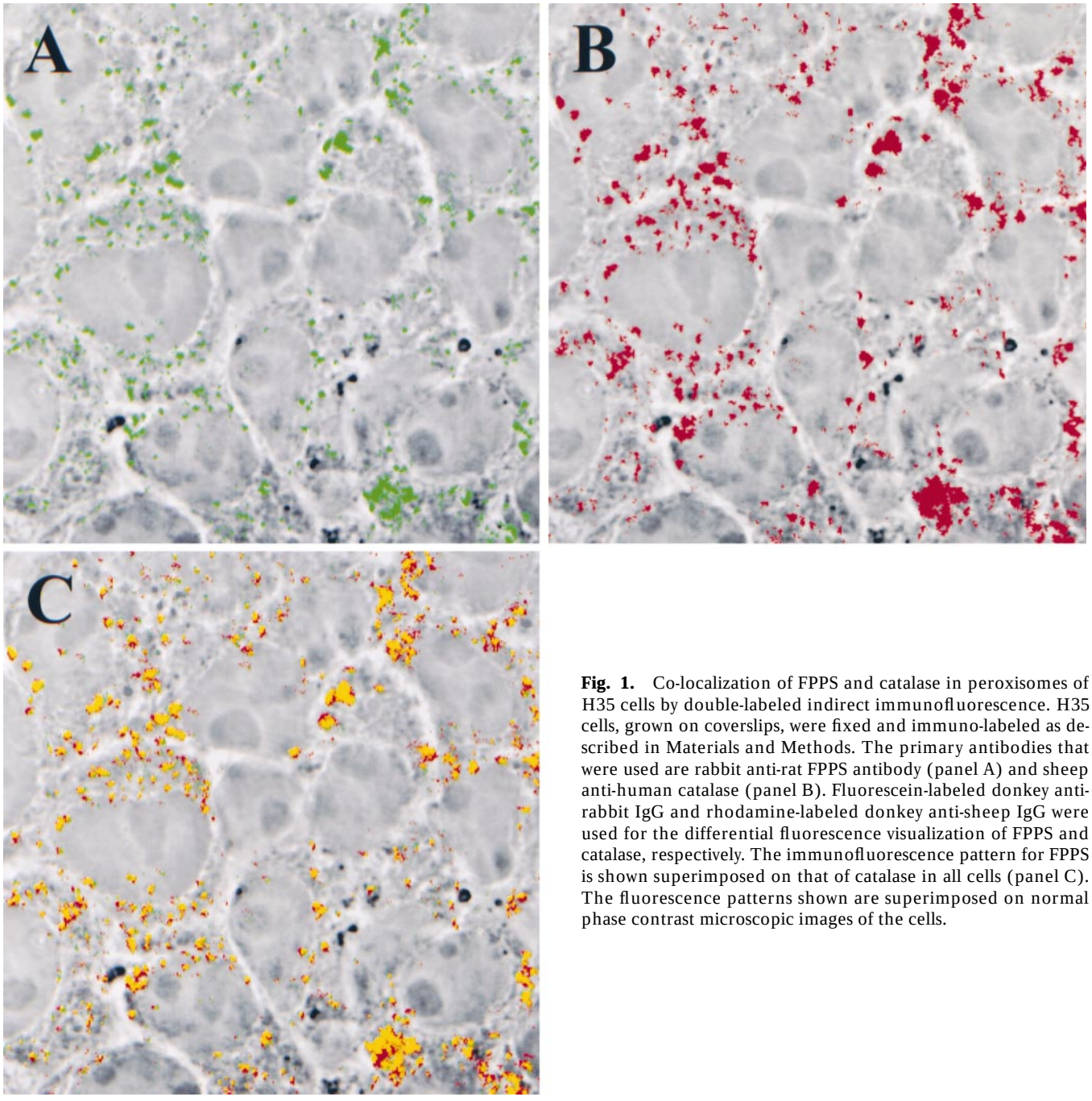

Fig. 1. Co-localization of FPPS and catalase in peroxisomes of H35 cells by double-labeled indirect immunofluorescence. H35 cells, grown on coverslips, were fixed and immuno-labeled as described in Materials and Methods. The primary antibodies that were used are rabbit anti-rat FPPS antibody (panel A) and sheep anti-human catalase (panel B). Fluorescein-labeled donkey anti-rabbit IgG and rhodamine-labeled donkey anti-sheep IgG were used for the differential fluorescence visualization of FPPS and catalase, respectively. The immunofluorescence pattern for FPPS is shown superimposed on that of catalase in all cells (panel C). The fluorescence patterns shown are superimposed on normal phase contrast microscopic images of the cells.

conjugated goat anti-rabbit IgG used at a dilution of 1:50. Cell sections were stained in an LKB ultra stainer (Leica, Inc., Deerfield, IL) for 20 min with uranyl acetate and 2 min with lead citrate. Sections were examined and photographed using a Phillips transmission electron microscope.

RESULTS

Localization of FPPS in H35 cell peroxisomes by indirect immunofluorescence microscopy

Indirect immunofluorescence microscopy studies by Krisans et al. (9) have shown that FPPS is localized in the peroxisomes of a variety of cells. However, subcellular fractionation studies found much of the activity in the cytosol. To substantiate the peroxisomal localization of FPPS in H35 cells, we have used subcellular fractionation and double immunofluorescence labeling. Preliminary studies involving subcellular fractionation of these cells resulted in the release of the majority of the FPPS activity into the cytosolic supernatant (data not shown) similar to the results shown by Krisans et al. (9). Double immunofluorescent labeling of cells with both anti-FPPS antibody (**Fig. 1A**) and anti-catalase antibody (Fig. 1B) yields a punctate immunofluorescence pattern for both enzymes typical of peroxisomal proteins (39). The immunofluorescence pattern of FPPS superimposes the pattern of catalase, a known peroxisomal enzyme (Fig. 1C) supporting the colocalization of the two enzymes in peroxisomes.

Time course release of FPPS from H35 cells during digitonin permeabilization

The observed FPPS colocalization with catalase as determined by indirect immunofluorescence contradicts the subcellular fractionation data showing the release of the majority of FPPS activity with the cytosol. Digitonin treatment of cells has been reported to reversibly permeabilize the plasma membrane while leaving subcellular organelles intact (35, 40). Therefore, we have used digitonin permeabilization of H35 cells to further characterize the subcellular localization of FPPS. The time course release of the cellular enzymes, lactate dehydrogenase (LDH), a cytosolic marker, catalase, a peroxisomal marker, and FPPS as well as cellular protein is shown in **Fig. 2**. Most of the release of proteins from the permeabilized cells occurs within 6 min and is complete after 14 min of treatment. At this time, all of the activity of LDH and about 57% of the cellular protein are released. However, catalase activity is fully retained in the permeabilized cells indicating that the peroxisomes remained intact. Interestingly, 67% of the FPPS activity released plateaued after 6 min incubation time, and only 33% is retained after 14 min permeabilization treatment. The digitonin-free buffer washes of the non-permeabilized control cells contained only 3% of the FPPS activity present in these cells. Based on these kinetic studies, we chose a 9 min permeabilization period where cellular protein loss plateaus (Fig. 2).

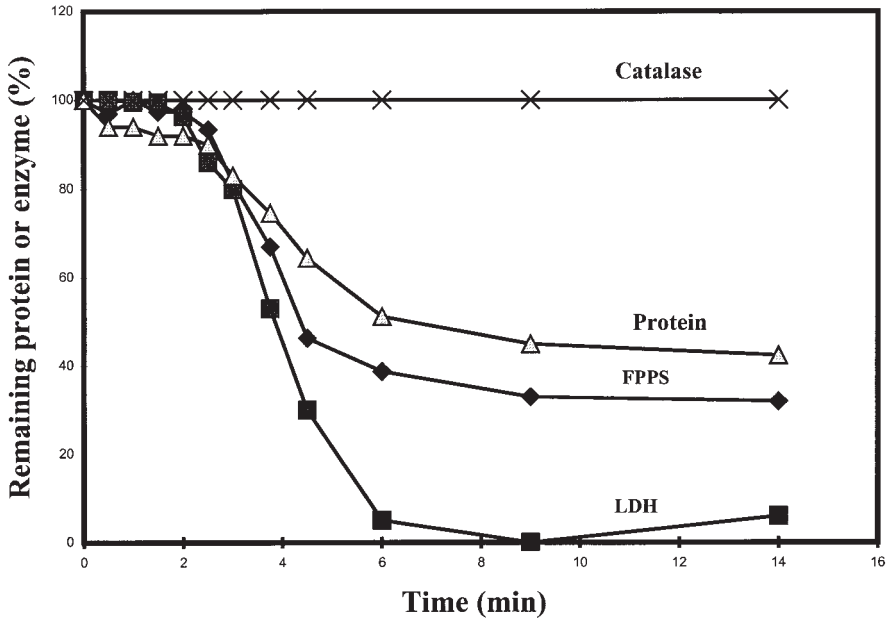

Fig. 2. Time course release of protein and enzymes from H35 cells during digitonin permeabilization. H35 cells, grown on 150 mm plates, were washed with ice-cold PBS, and permeabilized with buffer containing 40 μg/ml digitonin as described in Materials and Methods. At different incubation times, incubation buffer samples were collected and analyzed for protein and enzymatic activities of lactate dehydrogenase (LDH), catalase, and FPPS as described in Materials and Methods. Cells on control plates were treated with buffer without digitonin and samples were processed similarly. After 14 min, the incubation buffers were removed, cell extracts were prepared, and enzyme activities and protein were determined. The amount of protein or enzyme activities retained in cells from control plates is defined as 100%. The values are expressed as the percentage of total protein or enzyme activities remaining in the cells after permeabilization.

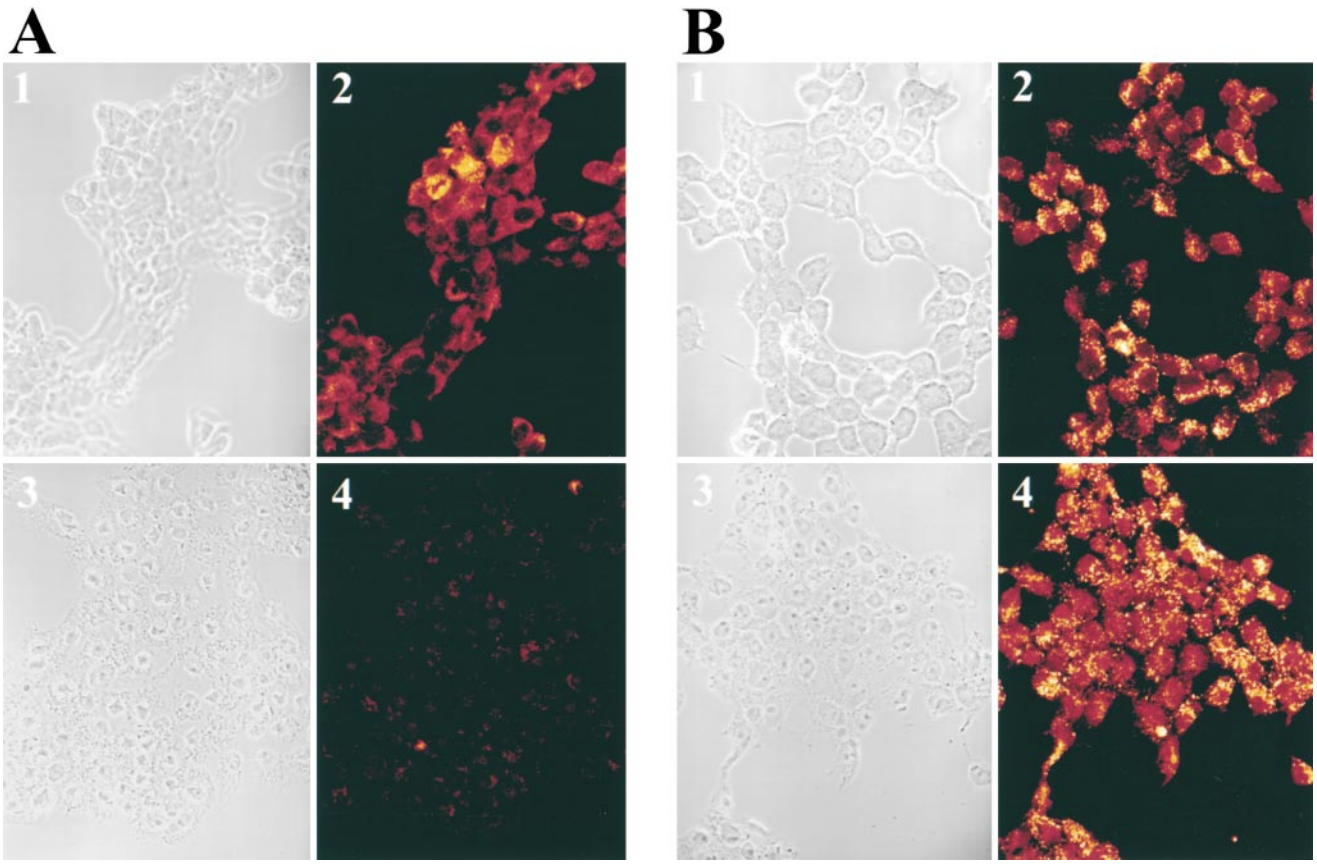

Fig. 3. Indirect immunofluorescent microscopy of FPPS and catalase in normal and permeabilized H35 cells. The cells grown on cover slips were permeabilized for 9 min and immuno-labeled for FPPS (part A) and catalase (part B) as described in Material and Methods. Immunofluorescent images were taken at different focal planes, 0.5 microns apart using a motorized stage. Selected frames are shown to demonstrate that normal (non-permeabilized) H35 cells contain both FPPS (A2) and catalase (B2). However, permeabilized cells, which are shown to contain enhanced fluorescence of catalase (B4), are devoid of most of the FPPS and only residual immunofluorescence can be detected (A4). Adjacent to each fluorescent image is the normal phase contrast microscopic images of the cells. The permeabilized cells (bottom) are flat and exhibit minimal phase contrast in comparison to normal cells (top).

Effect of permeabilization of H35 cells on the localization of FPPS

Figure 3 demonstrates the effect of permeabilization on the localization of both FPPS and catalase. As shown, both FPPS (Fig. 3A2) and catalase (Fig. 3B2) are present in intact cells. However, after permeabilization, most of the FPPS immunofluorescence disappears and only a faint remaining signal can be observed (Fig. 3A4), whereas catalase is retained and its immunofluorescence appears to be more concentrated (Fig. 3B4). Extensions of the permeabilization period or repeated cycles of permeabilization did not cause further decrease in the remaining fluorescence of either FPPS or catalase (data not shown). The effect of permeabilization on the localization of FPPS in H35 cells was also studied by indirect gold immunolabeling (38). Specific immunolabeling of FPPS was detected in the matrix of the peroxisomes in intact cells (**Fig. 4A**). Immuno-gold labeling was also observed in permeabilized cells but the number of particles was considerably lower than that observed in normal cells (Fig. 4B). Thus, these results also clearly indicated that FPPS is localized in peroxisomes, and a significant amount is released on permeabilization. The release of FPPS under these conditions was also demonstrated by Western blot analyses of fractions obtained from permeabilized cells (**Fig. 5**). As shown, non-permeabilized cells retained most of the FPPS protein whereas FPPS protein from permeabilized cells is observed mostly in the digitonin wash buffer (Fig. 5).

Selective release of HMG-CoA reductase, mevalonate kinase, and phosphomevalonate kinase from permeabilized H35 cells

Three additional enzymes, HMG-CoA reductase, mevalonate kinase, and phosphomevalonate kinase, involved in the early steps of the isoprenoid metabolic pathway were reported to be localized in peroxisomes (7). Therefore, we have examined the effect of digitonin permeabilization of H35 cells on these three enzymes. For these studies, we have used a 9-min permeabilization period at which cellular protein release plateaus (Fig. 2). The release of these three enzymes after permeabilization was compared to LDH and catalase which are shown in **Table 1**. Control cells treated with buffer lacking digitonin showed release of 8% and 16% of total cellular protein and LDH activity,

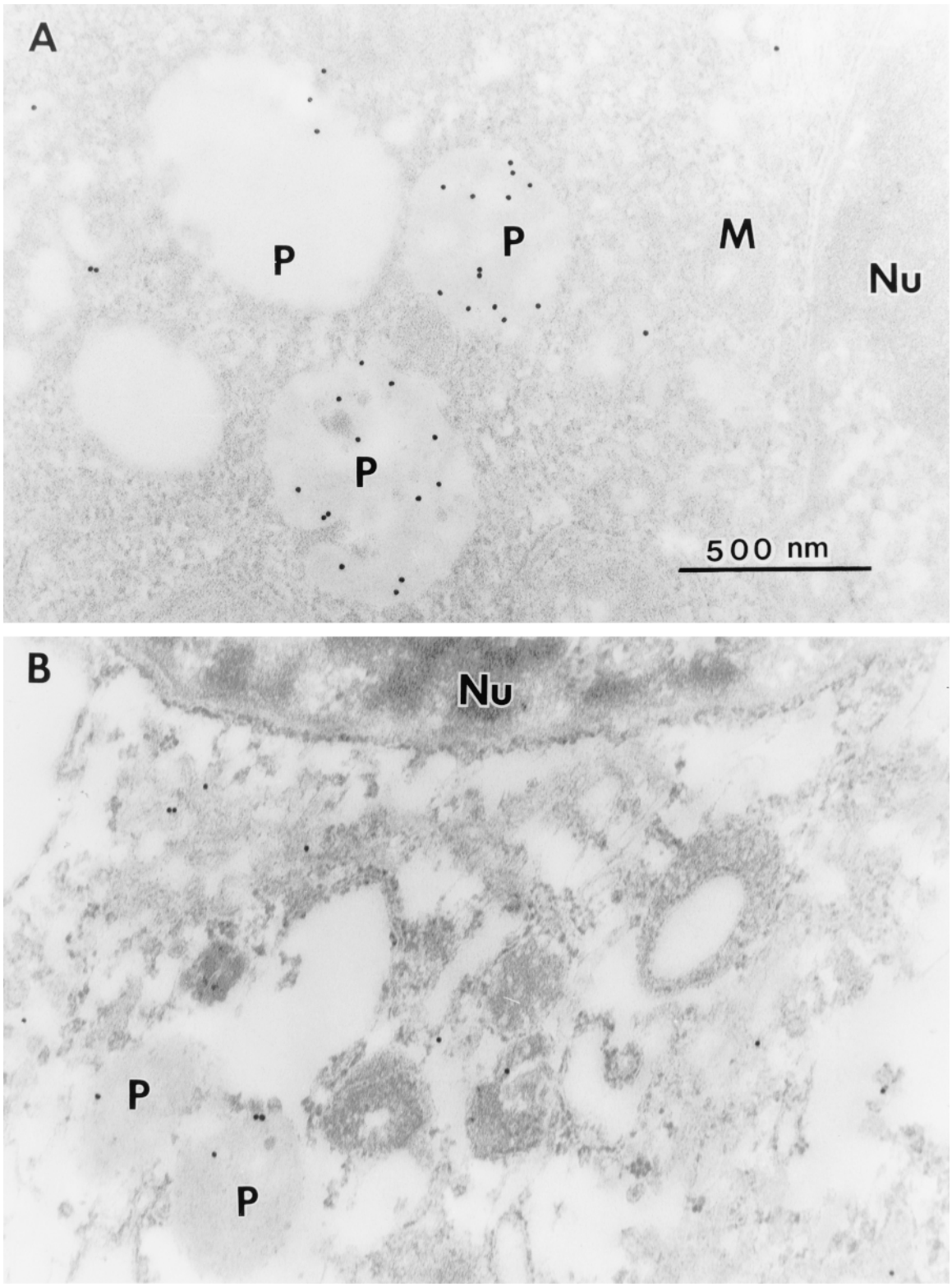

Fig. 4. Electron micrographs of normal and permeabilized rat Liver H35 cells. Cells were permeabilized with digitonin for 6 min as described in Materials and Methods, and fixed in 4% paraformaldehyde and 0.1% glutaraldehyde, without osmium tetroxide postfixation. Cell pellets were embedded in LR White. Sections were immunolabeled for FPPS using rabbit anti-rat antibody as the primary antibody, followed by gold-conjugated goat anti-rabbit IgG (15 nm gold particles). Sections were examined and photographed using a Phillips Transmission Electron Microscope. Most of the gold-labeled particles are localized in peroxisomes in normal cells (A). On permeabilization, the amount of gold labeling is decreased in peroxisomes (B). In control specimens, prepared as in "A" except that instead of primary antibody only BSA was used, gold labeling could not be observed (not shown). Nu, nucleus; M, mitochondria; P, peroxisomes; bar = 500 nm.

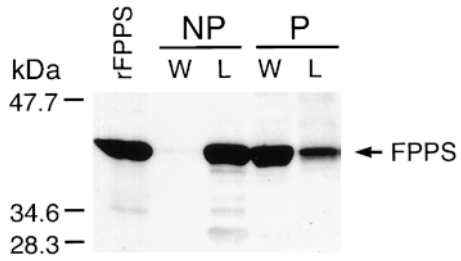

Fig. 5. Western blot analysis of FPPS in normal and permeabilized H35 cells. H35 cells were permeabilized with digitonin or incubated with buffer without digitonin for 9 min, and cell lysates were prepared as described in Materials and Methods. Samples, each containing 30 μg protein (except that of the permeabilized cell lysate where 100 μg protein was used for better visualization) were applied onto the gel. Samples were separated by SDS PAGE, transferred to nitrocellulose membranes, and incubated with rabbit anti-rat FPPS IgG. The second antibody used for visualization was peroxidase-conjugated goat anti-rabbit. Most FPPS protein is retained in normal cells, whereas, substantial release is observed in permeabilized cells. NP, non-permeabilized cells; P, permeabilized cells; W, wash buffer; L, cell lysate; rFPPS, recombinant rat FPPS expressed in *E. coli*.

respectively. Total cellular protein and LDH activity released after digitonin treatment were 58% and 93%, respectively. Catalase activity is not released from the permeabilized cells and is retained in amounts equal to that of the normal cells. HMG-CoA reductase, known to be localized to the ER and peroxisomes (2–4), is fully retained, and similar to catalase, its activity is not released into the permeabilization buffer.

We have consistently observed that the total FPPS activity recovered from digitonin-treated cells is 40–50% higher than the activity recovered from normal cells. Direct addition of digitonin to the fractions of cell wash or cell lysate from non-permeabilized cells failed to further activate the enzyme (data not shown), indicating that the increase in FPPS activity is not a direct effect of the presence of digitonin on the enzyme in the extracts. Approximately 50% digitonin-induced increased recovery of total FPPS activity can be calculated from the data presented in Table 1. Whatever the explanation, here again, the majority of the FPPS activity is released from permeabilized cells, and only about 40% of the total activity is retained. Both mevalonate kinase and phosphomevalonate kinase are not retained after permeabilization with digitonin and the amount of each activity released was 95% and 91%, respectively. The data show that the examined peroxisomal enzymes display markedly different association with this organelle.

Localization of FPPS in the non-hepatic CHO-K1 and peroxisomal deficient mutant ZR-82 cell line

ZR-82 cells, a peroxisomal-deficient CHO mutant, were reported to lack normal peroxisomes and show reduced peroxisomal functions due to the deficiency of peroxisomal matrix enzymes (25, 26). Therefore, it was of interest to study the release of FPPS upon permeabilization of both CHO-K1 (wild-type) and ZR-82 cells. We first investigated the localization of FPPS in these two cell lines. Immunofluorescent patterns for catalase and FPPS are similar in non-permeabilized CHO-K1 cells. These two enzymes are co-localized as shown by the superimposed images (**Fig. 6D**). Indirect immunofluorescence of these two proteins in the peroxisome-deficient ZR-82 cells showed a different pattern than that observed in CHO-K1 cells (**Fig. 7**). The punctate pattern is no longer observed and immunofluorescence is seen evenly distributed throughout the cytosol. Furthermore, detailed examination showed that immunofluorescence of FPPS in these cells is not colocalized with that of catalase (Fig. 7D).

Preliminary permeabilization studies using CHO-K1 and ZR-82 cells showed that after 6 min incubation with digitonin LDH release was complete. Therefore, in the following experiments we used this time period. The release of enzymes and proteins after permeabilization of CHO-K1, and ZR-82 cells, are shown in **Table 2**. As expected, the cytosolic LDH activity is totally released from both cell lines by digitonin treatment. Catalase activity is fully retained in CHO cells with or without digitonin treatment. However, as expected, this activity is released from permeabilized ZR-82 cells because, like LDH, catalase also resides in the cytosol in this cell line. FPPS, although shown to be localized in peroxisomes, is fully released from CHO cells by digitonin treatment, and unlike in H35 cells no partial retention of activity is observed.

TABLE 1. Differential release of enzymes in the isoprenoid biosynthetic pathway by digitonin permeabilization of H35 cells

	Non-Permeabilized Cells			Permeabilized Cells		
	Cell Lysate	Cell Wash	% Release	Cell Lysate	Cell Wash	% Release
Protein (mg/plate)	4.70 ± 0.43	0.78 ± 0.19	16 ± 3	2.23 ± 0.64	3.02 ± 0.36	58 ± 5
Enzyme (units/plate)						
LDH	2.64 ± 0.62	0.23 ± 0.08	78 ± 1	0.28 ± 0.10	3.55 ± 0.96	93 ± 2
Catalase	34.3 ± 19	0	0	35 ± 9.2	0	0
FPPS	228 ± 129	5.0 ± 8.7	4.5 ± 8	136 ± 32	214 ± 57	60 ± 11
Mevalonate kinase	3.17 ± 0.74	0.12 ± 0.04	3.7 ± 0.3	0.12 ± 0.03	2.33 ± 0.51	95 ± 0
Phosphomevalonate kinase	0.20 ± 0.02	0	0	0.13 ± 0.06	1.17 ± 0.12	91 ± 4
HMG-CoA reductase	121 ± 38	0	0	103 ± 5	0	0

Cells were incubated in buffer in the presence or absence of digitonin for 9 min as described in Materials and Methods. Released enzyme activities (cell wash) and activities remaining in the cells (cell lysate) were measured. The values for protein and enzyme activities are the mean ± SD of three separate experiments each done in duplicate.

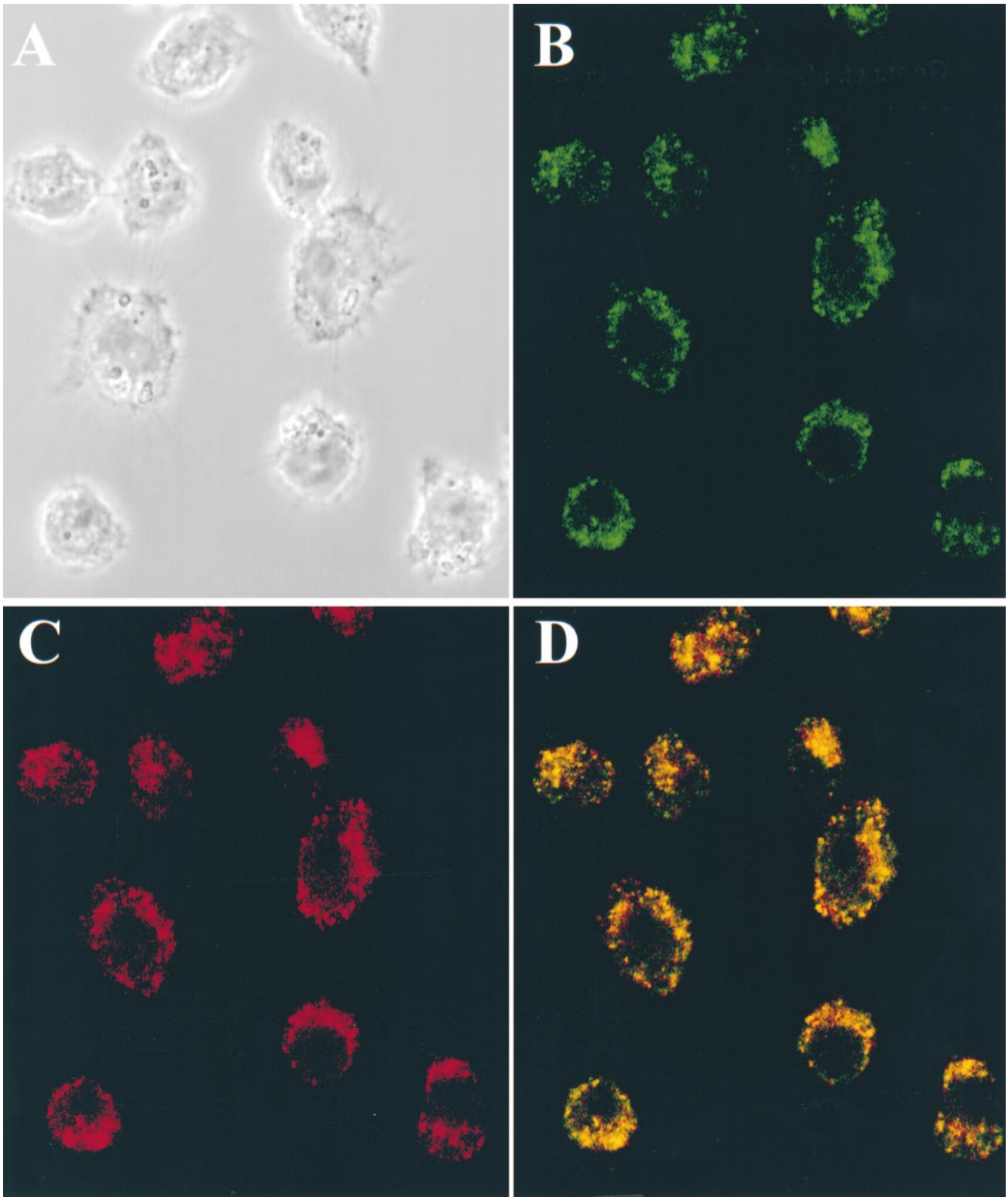

Fig. 6. Double-labeled indirect immunofluorescence microscopy of CHO K-1 cells. Cells grown on cover slips were fixed and treated as described in Materials and Methods. The cells were immunolabeled for catalase and FPPS simultaneously as described in the legend for Fig. 1. The punctated immunofluorescence pattern of FPPS (B) and catalase (C) are superimposable (D) indicating co-localization of the two enzymes. Panel A is the phase contrast micrograph of the same cells.

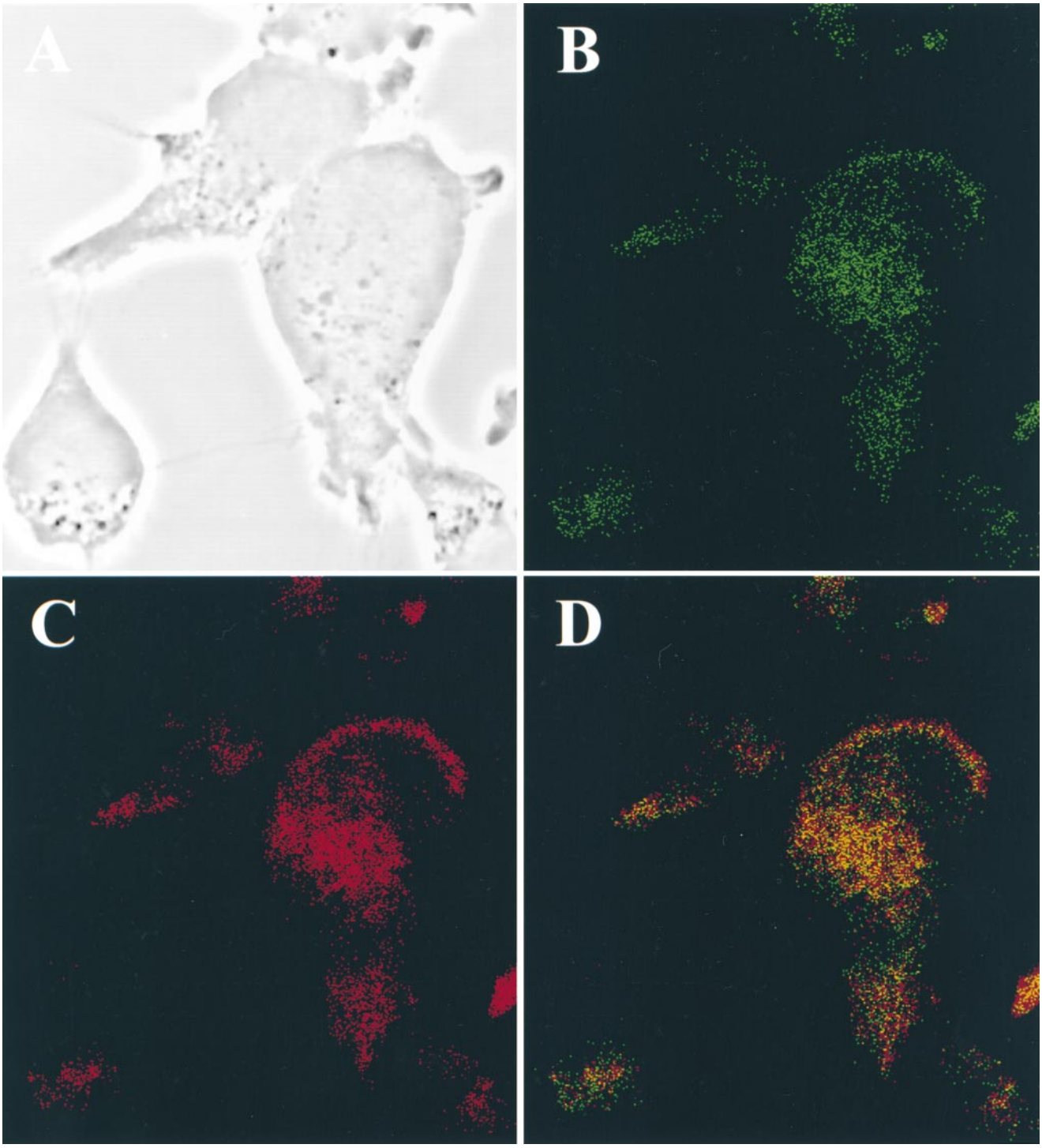

Fig. 7. Double-labeled indirect immunofluorescence microscopy of ZR-82 cells. Cells were grown and immunolabeled as described in the legend for Fig. 6. The immunofluorescence patterns of FPPS (B) and catalase (C) are typical of a cytosolic dispersion of these enzymes and are not superimposable (D). Panel A is the phase contrast micrograph of the same cells.

The release of FPPS by digitonin treatment in these cells was also confirmed by Western blot analyses. **Figure 8** depicts the release of FPPS from both permeabilized and normal CHO-K1 and ZR-82 cells. A major immunoreactive band corresponding to a protein of 41 kDa is observed. In both cell lines the major amount of FPPS is released upon permeabilization, in agreement with the results shown in Table 2. There is also a small release of FPPS from non-permeabilized cells which might have resulted on exposure of the cells to the buffer. Unlike the data in Table 2, both CHO-K1 and ZR-82 cells retain imunoreactive material after permeabilization. This material may be due to the residual FPPS activity or, alternatively, represent inactive enzyme.

TABLE 2. Protein and enzyme activities of LDH, catalase, and FPPS released from CHO-K1 and ZR-82 cells after digitonin permeabilization

	CHO-K1			ZR-82		
	Cell Lysate	Cell Wash	% Release	Cell Lysate	Cell Wash	% Release
Protein (mg/plate)	0.28 ± 0.03	2.11 ± 0.27	88.2 ± 0.3	0.42 ± 0.42	1.61 ± 0.69	90.5 ± 2.5
Enzyme (units/plate)						
LDH	0.07 ± 0.00	5.21 ± 0.00	98.7 ± 0.0	0.05 ± 0.07	4.26 ± 0.06	99.1 ± 1.3
Catalase	2.70 ± 0.00	0.00 ± 0.00	0.0 ± 0.0	0.00 ± 0.00	5.25 ± 0.00	100 ± 0.0
FPPS	3.55 ± 5.02	567 ± 397	99.5 ± 0.7	2.90 ± 2.91	507 ± 39	99.8 ± 0.3

Cells were incubated in buffer in the presence or absence digitonin for 6 min as described in Materials and Methods. Released enzyme activities (cell wash) and activities remaining in the cells (cell lysate) were measured. The values for protein and enzyme activities are the mean ± SD of three separate experiments each done in duplicate.

DISCUSSION

FPPS catalyzes two sequential 1′–4 condensation reactions of isopentyl diphosphate with the allylic diphosphates, dimethylallyl diphosphate, and geranyl diphosphate (41). The final product, FPP, is utilized in the synthesis of a large variety of isoprenoids such as squalene, cholesterol, farnesylated and geranylgeranylated proteins, dolichol, coenzyme Q, and the isoprenoid moiety of Heme A (12). Thus, the regulation of the formation and further conversion of FPP are important as variations in FPP levels and its availability to other metabolic pathways could alter its flux into sterol or nonsterol isoprenoid end products. Because the main flux of cellular isoprenoids is in sterol formation, the reported localization of FPPS in peroxisomes (9) leaves unclear the transport mechanism of FPP to squalene synthase, the next enzyme in this pathway, shown to be exclusively localized in the ER (10). Although it has been inferred that the site of FPP synthesis is in the peroxisomes due to the localization of its biosynthetic enzymes there (9), the actual site of formation of FPP is still unproven. Based on the available data, we cannot exclude a model in which the peroxisomes serve as a storage site for these enzymes where a small fraction of them are transported to and from the cytosol to generate FPP in proximity to the subcellular site where it is further metabolized. Therefore, we undertook the present study to assess the accessibility of these enzymes to the cytosol from intact peroxisomes. Subcellular fractionation of organelles causes relatively high damage to peroxisomes and allows leakage of matrix proteins such as catalase. We, therefore, have used cellular permeabilization techniques for our studies to fully preserve peroxisomal integrity.

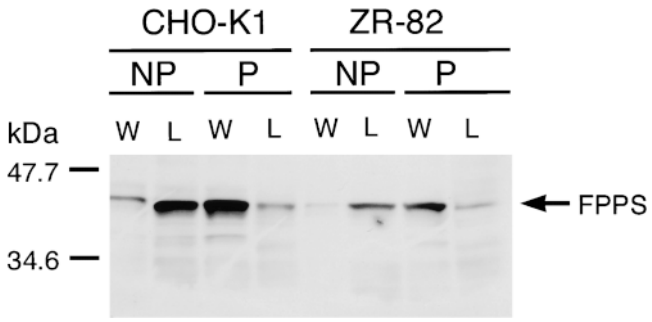

Fig. 8. Western blot analysis of FPPS in normal and permeabilized CHO-K1 and ZR-82 cells. Cells were permeabilized with digitonin or incubated with buffer without digitonin for 6 min and cell lysates were prepared as described in Materials and Methods. Samples, each containing 50 μg, were applied onto the gel. Samples were separated by SDS PAGE, transferred to nitrocellulose membranes, and incubated with rabbit anti-rat FPPS IgG. The second antibody used for visualization was peroxidase-conjugated goat anti-rabbit. Most FPPS protein is retained in normal cells whereas substantial release is observed in permeabilized cells. NP, non-permeabilized cells; P, permeabilized cells; W, wash buffer; L, cell lysate.

The indirect immunofluorescence (Figs. 1, 3, and 6) and immunoelectron microscopy (Fig. 4) show that most of the FPPS protein is co-localized with catalase in the lumen of the peroxisomes in the hepatic H35 cells and the non-hepatic CHO-K1 cells, similar to the observations reported for the non-hepatic human breast cancer (SKB-R-3) and CV-1 cells (9). As expected, in ZR-82 mutant cells that lack functional peroxisomes due to the deficiency in peroxisome assembly factor (25), both FPPS and catalase are distributed in the cytosol (Fig. 7B, C, and D).

Digitonin permeabilization of H35 cells results in a loss of about 70% of the FPPS activity to the permeabilization buffer. Under these conditions there is a complete efflux of cytosolic LDH, indicating high permeabilization efficiency. However, catalase activity is fully retained in the cells which indicates retention of peroxisomal integrity (Fig. 2 and Fig. 3 B4). It is interesting to note that a significant fraction of FPPS is reproducibly retained in H35 cells after permeabilization (Fig. 2). This is also substantiated by the Western blot analyses (Fig. 5), by a faint, yet detectable residual immunofluorescence signal (Fig. 3 A4), and by a retention of a residual immuno-gold labeling in electron microscopy in permeabilized cells (Fig. 4 B). These four independent determinations suggest that there are two distinct pools of FPPS protein in H35 cells: one which is readily diffused out of the peroxisomes, and the second which is retained within the cells following permeabilization. The analysis used cannot determine whether the two pools consist of different proteins as they exhibit the same size and migrate with the same pI in isoelectric focusing gel (data not shown). In contrast, practically all the FPPS activity (99%) escapes from CHO-K1 cells under the same conditions (Table 2). This loss was also substantiated by indirect immunofluorescence in which no residual immunofluorescence could be detected

(data not shown). However, a significant band of FPPS is detected in Western blots of permeabilized CHO-K1 and ZR-82 cell lysates (Fig. 8). As cytosolic LDH activity is completely washed out from these permeabilized cells (Table 2), indicating a total loss of the cytosol, it may suggest the existence of a non-cytosolic, non-peroxisomal, inactive protein identical to or with the same size and immunocharacteristics as FPPS.

As expected, permeabilization of ZR-82 mutant cells also caused a complete loss of catalase activity that was found in the permeabilization medium. It also appears that ZR-82 mutant cells contain reduced levels of FPPS protein as compared to the wild-type CHO-K1 cells (Fig. 8). This could be related to the lack of peroxisomes in ZR-82 cells. Similar observations have been reported for other peroxisomal enzymes (5, 9). Mevalonate kinase from patients with peroxisomal deficiency disease (5) and HMG-CoA reductase in peroxisomal-deficient CHO cell lines (31) are found in reduced amounts.

In addition to FPPS, two other peroxisomal enzymes, mevalonate kinase and mevalonate-phosphate kinase, are also released from permeabilized H35 cells. However, in contrast, HMG-CoA reductase is retained in these cells (Table 1). These findings are somewhat different from the observations reported by Biardi and Krisans (7) in permeabilized non-hepatic CV-1 cells. There it was reported that the activities of mevalonate kinase, phosphomevalonate kinase, and mevalonate-diphosphate decarboxylase are retained in permeabilized cells (7).

Our data do not explain the consistent high total activity of FPPS in the fractions obtained after digitonin permeabilization. This observation is interesting as addition of digitonin itself failed to affect FPPS activity in the soluble extract obtained from non-permeabilized cells. Therefore, the activation cannot be a direct effect of digitonin on the enzyme or by removal of an inhibitor. Future studies will examine the interesting possibility that digitonin treatment of the cells may extract an activator molecule which, together with the enzyme, is responsible for the high FPPS activity observed.

Similar to our observations, it has been shown that HMG-CoA reductase was not released from permeabilized MET-18b-2 cells (42) or wild-type CHO-K1 cells (31). As about 50% of HMG-CoA reductase was released from ZR-78 and ZR-82 mutant cell lines, it was suggested that the peroxisomal HMG-CoA reductase was released (31). Based on these observations Krisans et al. (9) suggested that FPP synthesis occurs predominantly in peroxisomes. Subsequently, FPP is transported out of the peroxisomes for further metabolism in other organelles, is utilized further within the peroxisomes, or is converted to farnesol which is transported from the peroxisome (1). Our findings that the peroxisomal enzymes, mevalonate kinase, phosphomevalonate kinase, and FPPS, are readily released from permeabilized cells, may provide an alternate mechanism for the controlled synthesis of FPP and its distribution into different biosynthetic pathways localized in the different subcellular compartments. In this proposed mechanism the cells may control FPP synthesis by a reversible transport of enzymes from a centralized peroxisomal pool to the cytosolic compartment and thus, enabling the synthesis of FPP in the cytosol, in close proximity to the different cellular compartments in which it is utilized. Our findings do not eliminate (or support) an additional possibility that enzymes transported from the peroxisomes, under physiological conditions, may physically associate with target organelles to enable the further conversion of nascent FPP to various isoprenoid end products.

The mechanism of FPPS transport in and out of peroxisomes is an additional interesting topic that the data presented here cannot elucidate. It is clear that the efflux of the enzyme from peroxisomes under permeabilization conditions is not an energy-requiring process as it takes place at low temperature. Therefore, we can assume that the retention of FPPS in peroxisomes is either an energy-requiring process or it occurs by binding to a carrier in the peroxisomes, most likely a protein, which is also removed by the digitonin. Future studies, including possible enzyme modification, should elucidate this question.

We thank Mr. T. Baginski for the help in operating the confocal microscope and Dr. J. Czege for processing the images on computer at the USUHS, BIC facilities, and Dr. T. M. Martensen for useful editing support. This work was supported by National Institutes of Health Grants HL48540 and HL50628.

Manuscript received 5 March 1999 and in revised form 3 May 1999.

REFERENCES

1. Krisans, S. 1996. Cell compartmentalization of cholesterol biosynthesis. *Ann. NY Acad. Sci.* **804:** 142–164.
2. Keller, G. A., M. Pazirandeh, and S. Krisans. 1986. 3-Hydroxy-3-methylglutaryl-coenzyme A reductase localization in normal rat liver peroxisomes and microsomes of control and cholestyramine-treated animals: quantitative biochemical and immunoelectron microscopic analysis. *J. Cell Biol.* **103:** 875–886.
3. Keller, G. A., M. C. Barton, D. J. Shapiro, and S. J. Singer. 1985. 3-Hydroxy-3-methylglutaryl- coenzyme A reductase is present in peroxisomes in normal rat liver cells. *Proc. Natl. Acad. Sci. USA.* **82:** 770–774.
4. Engfelt, W. H., J. E. Shackelford, N. Jessani, N. Aboushadi, K. Masuda, V. G. Paton, G. A. Keller, and S. K. Krisans. 1997. The characterization of the UT-2 cells. The induction of peroxisomal 3-hydroxy-3-methylglutaryl-coenzyme A reductase. *J. Biol. Chem.* **272:** 24579–24587.
5. Biardi, L., A. Sreedhar, A. Zokaei, N. B. Vartak, R. Bozeat, J. E. Shackelford, G. A. Keller, and S. K. Krisans. 1994. Mevalonate kinase is predominantly localized in peroxisomes and is defective in patients with peroxisome deficiency disorders. *J. Biol. Chem.* **269:** 1197–1205.
6. Stamellos, K. D., J. E. Shackelford, R. D. Tanaka, and S. K. Krisans. 1992. Mevalonate kinase is localized in rat liver peroxisomes. *J. Biol. Chem.* **267:** 5560–5568.
7. Biardi, L., and S. K. Krisans. 1996. Compartmentalization of cholesterol biosynthesis: conversion of mevalonate to farnesyl diphosphate occurs in the peroxisomes. *J. Biol. Chem.* **271:** 1784–1788.
8. Palton, V. G., J. E. Shackelford, and S. K. Krisans. 1997. Cloning and subcellular localization of hamster and rat isopentenyl diphosphate dimethylallyl diphosphate isomerase: a PTS1 motif targets the enzyme to peroxisomes. *J. Biol.Chem.* **272:** 18945–18950.
9. Krisans, S. K., J. Ericsson, P. A. Edwards, and G. A. Keller. 1994. Farnesyl-diphosphate synthase is localized in peroxisomes. *J. Biol. Chem.* **269:** 14165–14169.
10. Stamellos, K. D., J. E. Shackelford, I. Shechter, G. Jiang, D. Conrad, G. A. Keller, and S. K. Krisans. 1993. Subcellular localization

of squalene synthase in rat hepatic cells: biochemical and immunochemical evidence. *J. Biol. Chem.* **268:** 12825–12836.
11. Appelkvist, E. L., M. Reinhart, R. Fisher, J. Billheimer, and G. Dallner. 1990. Presence of individual enzymes of cholesterol biosynthesis in rat liver peroxisomes. *Arch. Biochem. Biophys.* **282:** 318–325.
12. Goldstein, J. L., and M. S. Brown. 1990. Regulation of the mevalonate pathway. *Nature.* **343:** 425–430.
13. Levy, B. D., N. A. Petasis, and C. N. Serhan. 1997. Polyisoprenyl phosphate in intracellular signalling. *Nature.* **389:** 985–990.
14. Spear, D. H., J. Ericsson., S. M. Jackson, and P. A. Edwards. 1994. Identification of a 6-base pair element involved in the sterol-mediated transcription regulation of farnesyl diphosphate synthase. *J. Biol. Chem.* **269:** 25212–25218.
15. Jackson, S. M., J. Ericsson, T. F. Osborn, and P. A. Edwards. 1995. NF-Y has a novel role in sterol-dependent transcription of two cholesterogenic genes. *J. Biol. Chem.* **270:** 21445–21448.
16. Jackson, S. M., J. Erickson, J. E. Metherall, and P. A. Edwards. 1996. Role of sterol regulatory element binding protein in the regulation of farnesyl diphosphate synthase and in the control of cellular levels of cholesterol and triglyceride: evidence from sterol regulation-defective cells. *J. Lipid Res.* **37:** 1712–1721.
17. Erickson, J., S. M. Jackson, B. C. Lee, and P. A. Edwards. 1996. Sterol regulatory element binding protein binds to a *cis* element in the promoter of the farnesyl diphosphate synthase gene. *Proc. Natl. Acad. Sci. USA.* **93:** 945–950.
18. Jiang, G., T. L. McKenzie, D. G. Conrad, and I. Shechter. 1993. Transcriptional regulation by lovastatin and 25-hydroxycholesterol in HepG2 cells and molecular cloning and expression of the cDNA for the human hepatic squalene synthase. *J. Biol. Chem.* **268:** 12818–12824.
19. Guan, G., G. Jiang, R. L. Koch, and I. Shechter. 1995. Molecular cloning and functional analysis of the promoter of the human squalene synthase gene. *J. Biol. Chem.* **270:** 21958–21965.
20. Guan, G., P. Dai, T. F. Osborne, J. B. Kim, and I. Shechter. 1997. Multiple sequence element are involved in the transcriptional regulation of the human squalene synthase gene. *J. Biol. Chem.* **272:** 10295–10302.
21. Guan, G., P. Dai, J. B. Kim, and Shechter, I. 1998. Differential transcriptional regulation of the human squalene synthase gene by sterol regulatory element-binding proteins (SREBP) 1a and 2 and involvement of 5′ DNA sequence element in the regulation. *J. Biol. Chem.* **273:** 12526–12535.
22. Novikoff, A. B., P. M. Novikoff, C. Davis, and N. Quintana. 1973. Studies on microperoxisomes. V. Are microperoxisomes ubiquitous in mammalian cells? *J. Histochem. Cytochem.* **21:** 737–755.
23. Lazarow, P. B., and H. W. Moser. 1995. Disorders of peroxisome biogenesis. *In* The Metabolism and Molecular Basis of Inherited Disease. C. R. Scriver, A. L. Beaudet, W. S. Sly, and D. Valle, editors. McGraw-Hill, Inc., New York. 2287–2324.
24. Shimozawa, N., T. Tsukamoto, Y. Suzuki, T. Orii, Y. Shirayoshi, T. Mori, and Y. Fujiki. 1992. A human gene responsible for Zellweger syndrome that affects peroxisomes. *Science.* **350:** 1132–1134.
25. Zoeller, R. A., and C. R. H. Raetz. 1986. Isolation of animal cell mutants deficient in plasmalogen biosynthesis and peroxisome assembly. *Proc. Natl. Acad. Sci. USA.* **83:** 5170–5174.
26. Zoeller, R. A., L. H. Allen, M. J. Santos, P. B. Lazarow, T. Hashimoto, A. M. Tartakoff, and C. R. H. Raetz. 1989. Chinese hamster ovary cell mutants defective in peroxisomes assembly. Comparison to Zellweger syndrome. *J. Biol. Chem.* **264:** 21872–21878.
27. Tsukamoto, T., S. Yokota, and Y. Fujiki. 1990. Isolation and characterization of CHO cell mutants defective in assembly of peroxisomes. *J. Cell Biol.* **110:** 651–660.
28. Tsukamoto, T., S. Miura, and Y. Fujiki. 1991. Restoration by a 35K membrane protein of peroxisome assembly in a peroxisome-deficient mammalian cell mutant. *Nature.* **350:** 77–81.
29. Thieringer, R., and C. R. H. Raetz. 1993. Peroxisome-deficient Chinese hamster ovary cells with point mutation in peroxisome assembly factor-1. *J. Biol Chem.* **268:** 12631–12636.
30. Van den Bosch, H., R. B. H. Schutgens, R. J. A. Wanders, and J. M. Tager. 1992. Biochemistry of peroxisomes. *Annu. Rev. Biochem.* **61:** 157–197.
31. Aboushadi, N., and S. K. Krisans. 1998. Analysis of isoprenoid biosynthesis in peroxisomal-deficient Pex2 CHO cell lines. *J. Lipid Res.* **39:** 1781–1791.
32. Shapiro, D. J., J. L. Nordstrom, J. J. Mitschelen, V. W. Rodwell, and R. T. Schimke. 1974. Microassay for 3-hydroxy-3-methylglutaryl-coenzyme A reductase in rat liver and in L-cell fibroblasts. *Biochim. Biophys. Acta.* **370:** 369–377.
33. Panini, S. R., R. Schnitzer-Polokoff, T. A. Spencer, and M. Sinensky. 1989. Sterol-independent regulation of 3-hydroxy-3-methylglutaryl-coenzyme A reductase by mevalonate in Chinese hamster ovary cells. *J. Biol. Chem.* **264:** 11044–11052.
34. Baudhuim, P., H. Beaufay, Y. Rahman-Li, Q. J. Sellinger, R. Wattiaux, P. Jaques, and C. de Duve. 1964. Tissue fractionation studies. 17. Intracellular distribution of monoamine oxidase, asparatate aminotransferase, alanine aminotransferase, d-amino acid oxidase and catalase in rat liver tissues. *Biochem. J.* **92:** 179–184.
35. Plutner, H., H. W. Davidson, J. Sarate, and W. E. Balch. 1992. Morphological analysis of protein transport from the ER to Golgi membrane in digitonin-permeabilized cells: role of P58 containing compartment. *J. Cell Biol.* **119:** 1097–1116.
36. Clarke, C. F., R. D. Tanaka, K. Svenson, M. Wamsley, A. M. Fogelman, and P. A. Edwards. 1987. Molecular cloning and sequence of a cholesterol-repressible enzyme related to prenyl-transferase in the isoprene biosynthetic pathway. *Mol. Cell. Biol.* **7:** 3138–3146.
37. Laemmli, U. K. 1970. Cleavage of structural proteins during the assembly of the head of bacteriophage T4. *Nature.* **227:** 680–685.
38. Goping, G., S. Yedgar, H. B. Pollard, and A. J. Kuijpers. 1992. Flat embedding and immunolabeling of SW 1116 colon carcinoma cells in LR White: an improved technique in light and electron microscope. *Microsc. Res. Tech.* **21:** 1–9.
39. Gould, S. J., S. K. Krisans, G. A. Keller, and S. Subramani. 1990. Antibodies directed against the peroxisomal targeting signal of firefly luciferase recognize multiple mammalian peroxisomal proteins. *J. Cell Biol.* **110:** 27–34.
40. Katz, J., and P. A. Wals. 1985. Studies wih digitonin-treated rat hepatocytes (nude cells). *J. Cell. Biochem.* **28:** 207–228.
41. Rilling, H. C., and L. T. Chayet. 1985. *In* Sterols and Bile Acids. H. Danielsson, and J. Stovall, editors. Elsevier Scientific Publishing Co., Inc., New York. 17–23.
42. Correll, C. C., L. Ng, and P. A. Edwards. 1994. Identification of farnesol as the non-sterol derivative of mevalonic acid required for the accelerated degradation of 3-hydroxy-3-methylglutaryl-coenzyme A reductase. *J. Biol. Chem.* **269:** 17390–17393.